Fracture of piezoelectric materials with the X-FEM

Eric Béchet* — Matthias Scherzer — Meinhard Kuna****

** Laboratoire de Physique et Mécanique des Matériaux*
Université de Metz
UMR CNRS 7554, Ile du Saulcy
F-57045 Metz cedex 1, France
eric.bechet@univ-metz.fr

*** Institut für Mechanik und Fluiddynamik*
TU Bergakademie Freiberg Lampadiusstrasse 4
09596 Freiberg, Germany
meinhard.kuna@imfd.tu-freiberg.de

ABSTRACT. *We present an application of X-FEM to the fracture analysis of piezoelectric materials. These materials are increasingly used in actuators and sensors. Under in service loading, phenomena of crack initiation and propagation may occur due to high electromechanical field concentrations. In the past few years, the extended finite element method (X-FEM) has been applied mostly to model cracks in structural materials. The present paper focuses on the definition of new enrichment functions suitable for cracks in piezolectric structures. The approach is based on specific asymptotic crack tip solutions, derived for piezoelectric materials.*

RÉSUMÉ. *On présente une application de X-FEM pour la mécanique de la rupture dans les matériaux piezoélectriques. Ces matériaux sont de plus en plus utilisés dans les actuateurs et les senseurs. Sous charges de service, des phénomènes d'initiation de fissure et de propagation peuvent se produire à cause des concentrations de contraintes électromécaniques. Dans les années passées, la méthode X-FEM a été appliquée majoritairement à des matériaux structuraux isotropes. Le présent article se concentre sur la définition de fonctions d'enrichissement adaptées aux matériaux piezoélectriques.*

KEYWORDS: *piezoelectric materials, crack, finite elements, X-FEM.*

MOTS-CLÉS : *matériaux piezoélectriques, fissure, éléments finis, X-FEM.*

DOI:10.3166/REMN.17.637-649

1. Introduction

Materials showing a strong piezoelectric effect are used in many applications, where they serve as sensors, actuators or transducers. Knowledge of the fracture behavior for these smart materials is often crucial within the design of parts under high electrical and mechanical loading. The Extended Finite Element Method (X-FEM) (Moës *et al.*, 1999) has been originally designed for crack growth analysis in isotropic elastic materials. In association with level-sets (Osher *et al.*, 1988) as a mean for representing the crack geometry, it is a powerful way to get rid of the costly constrained remeshing needed with conventional finite element techniques. Under certain circumstances, this method is also able to achieve regular convergence rates in the energy error even for a cracked domain.

Piezoelectric materials exhibit a coupling between mechanical and electrical variables, as well as transversely isotropic material characteristics. To treat this new problem in the extended finite element method, specific crack analysis tools and changes in the enrichment functions are needed, which allow to represent the crack - both in the mechanical and electrical functional spaces. It is worth noting that the methodology presented here may be applied to anisotropic elastic materials such as composites as well, though the conclusions drawn here may not apply to these.

2. Piezoelectric model

We recall here the linear material equations of piezoelectricity under the assumption of small strains. The cracked domain is denoted by Ω and its boundary $\partial\Omega \cup C^+ \cup C^-$ by B. The boundary B is subjected to specific boundary conditions: At the part B_n tractions or the electric field are imposed (natural boundary conditions), whereas at part B_e the displacement u_i or the electrical potential φ are prescribed (essential boundary conditions). The crack faces C^+ and C^- are assumed to be both traction-free and electrically impermeable.

$$\left.\begin{array}{l}\sigma_{ij}n_j = 0\\ D_i n_j = 0\end{array}\right\} \text{ on } C^- \cup C^+ \qquad [1]$$

$$\left.\begin{array}{l}\sigma_{ij}n_j = t_j\\ D_i n_j = q\end{array}\right\} \text{ on } B_n \qquad [2]$$

$$\left.\begin{array}{l}u_i = u_i^0\\ \varphi = \varphi^0\end{array}\right\} \text{ in } B_e \qquad [3]$$

The Cauchy stress tensor σ_{ij} and the electric displacement D_j must satisfy the equilibrium equations:

$$\left.\begin{array}{l}\sigma_{ij,j}=0\\ D_{j,j}=0\end{array}\right\} \text{ on } \Omega \quad [4]$$

The strain ε_{ij} and electric field E_j are derived from displacement u_i and electric potential φ:

$$\varepsilon_{ij} = \frac{1}{2}(u_{i,j}+u_{j,i}) \quad [5]$$

$$E_j = -\varphi_{,j} \quad [6]$$

The constitutive law is defined by:

$$\sigma_{ij} = c_{ijkl}\varepsilon_{kl} - e_{kij}E_k \quad [7]$$

$$D_i = e_{ikl}\varepsilon_{kl} + \kappa_{ik}E_k \quad [8]$$

where c_{ijkl} is Hooke's elasticity tensor, κ_{ij} is the dielectric tensor and e_{ijk} is the piezoelectric tensor. These tensors are known experimentally for various piezoelectric materials. They are usually anisotropic.

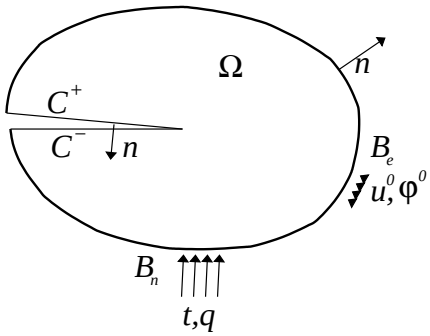

Figure 1. *Cracked body with boundary conditions*

3. Analytical solutions

In the following, analytical eigenfunction expansions will be recalled for a semi-infinite crack in an infinite piezoelectric domain. The asymptotic expansion will be used to generate the set of enrichment functions that span the exact solution at crack tips for any remote loading case. In addition, we will present the analytic solution for a Griffith crack in an infinite domain. The

latter will be used in the sequel to compare enrichment strategies by evaluating the convergence rate for an increasing refinement of the finite element mesh. For a detailed description of the analytical functions, please refer to (Béchet *et al.*, 2008).

3.1. *Asymptotic expansion for a semi-infinite crack*

In order to make the paper self-contained, we will briefly look back on the extraction of the asymptotic eigenfunction expansion at crack tips in piezoelectric materials. The details can be found, for instance, in (Scherzer *et al.*, 2004; Suo *et al.*, 1992). Thus, the concrete forms of the general equations [1] to [8] for their application in the X-FEM will be derived. We will restrict our analysis to plane strain conditions ($\varepsilon_{xz} = \varepsilon_{yz} = \varepsilon_{zz} = E_z = 0$) for transversely isotropic piezoelectrics with respect to the material axes x and y (poling direction) as considered in (Sosa, 1991). Let us now consider the general solution of the piezoelectric boundary value problem within an infinite domain based on the coordinates x and y (poling axis). Introducing the potentials $U(x, y)$ and $\chi(x, y)$ (Sosa, 1991) with the definitions

$$\sigma_{xx} = U(x,y)_{,yy}, \qquad \sigma_{yy} = U(x,y)_{,xx}, \qquad \sigma_{xy} = -U(x,y)_{,xy} \qquad [9]$$

$$D_x = \chi(x,y)_{,y}, \qquad D_y = -\chi(x,y)_{,x} \qquad [10]$$

, the general solution for $U(x, y)$ is built-up by means of the six roots $a_1, a_2, ..., a_6$. They follow from the characteristic equation for a through the linear combination

$$U(x,y) = \sum_{i=1}^{6} U_i(x + a_i y). \qquad [11]$$

The $U_i(z_i)$ in [11] are arbitrary functions of $z_i = x + a_i y$. It is clear that $\chi(x, y)$ has the same structure as $U(x, y)$ in [11] with the corresponding functions $\chi_i(z_i)$.

In the next step we seek for the solution around the tip of a straight crack in an infinite plane, see Fig. 2. To allow for arbitrary poling directions, the material coordinate system (x, y) is rotated by an angle α with respect to the crack axis. In order to fulfil the boundary conditions at crack faces, it is necessary and convenient to expand the general solution in Laurent-like series using general power functions for $U_i(z_i)$ (see e.g. (Mußchelichwili, 1971)). The origin of the coordinates x and y is taken at the crack tip:

$$U(x,y) = \sum_{k} \sum_{i=1}^{6} d_i(\lambda_k)(x + a_i y)^{\lambda_k + 2} \qquad [12]$$

The complex variables $d_i(\lambda_k)$ are free coefficients of the series expansion at the crack tip. They can be determined only from the overall solution of the considered boundary value problem. The values λ_k are generally complex.

In order to fulfil the classical homogeneous boundary conditions, one has to represent the stress function, the stresses and the dielectric displacements in a polar coordinate system (r, θ) with $\theta = 0$ at the crack prolongation ligament as it is usually assumed. Another point consists in the fact that the material properties considered give six characteristic roots $a_1, a_2, ..., a_6$ representing three conjugate complex pairs. Owing to the real property of $U(x, y) = U(r, \theta)$, the corresponding terms of a_i and $\overline{a_i}$ in [12] have to be combined mutually for real λ_k. Finally, one gets for each pair of a_i and $\overline{a_i}$ $(i = 1, 2, 3)$ in [12] expressions for the stress function U in polar coordinates r and $\omega = \theta - \alpha$ of the form:

$$
\begin{aligned}
&e_i p^{\lambda_k+2} \cos\left[(\lambda_k+2)(\kappa+\tfrac{\pi}{2})\right] + f_i p^{\lambda_k+2} \sin\left[(\lambda_k+2)(\kappa+\tfrac{\pi}{2})\right], \\
&\text{with } p = r\sqrt{(\cos\omega)^2 + a_i^{(\mathrm{re})} \sin(2\omega) + (\sin\omega)^2 \left[\left(a_i^{(\mathrm{im})}\right)^2 + \left(a_i^{(\mathrm{re})}\right)^2\right]}, \\
&\kappa = \arctan \frac{\cos(\omega) + a_i^{(\mathrm{re})} \sin(\omega)}{a_i^{(\mathrm{im})} \sin(\omega)} \\
&d_i(\lambda_k) = e_i(\lambda_k) + \mathrm{i} f_i(\lambda_k), \quad a_i = a_i^{(\mathrm{re})} + \mathrm{i} a_i^{(\mathrm{im})}
\end{aligned}
\qquad [13]
$$

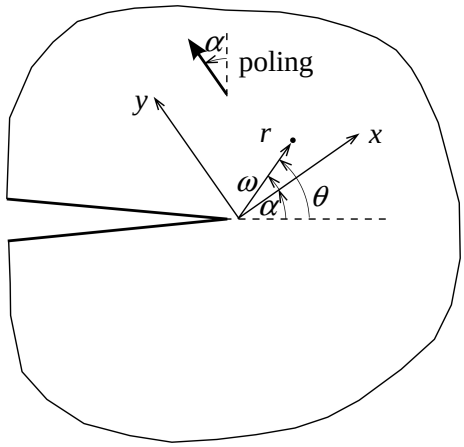

Figure 2. *Definition of the material axes around the crack tip*

All mechanical and electrical variables can be calculated only by means of the potential $U(x, y)$. For the considered homogeneous crack face boundary conditions one gets for λ_k the values:

$$\lambda_1 = -\frac{1}{2},\ \lambda_2 = 0,\ \lambda_3 = \frac{1}{2},\ \lambda_4 = 1,\ \lambda_5 = \frac{3}{2},\ \ldots \qquad [14]$$

The root $\lambda_1 = -\frac{1}{2}$ generates three independent eigenvectors based on the coefficients $e_1(\lambda_1)$, $f_1(\lambda_1)$, $e_2(\lambda_1)$, $f_2(\lambda_1)$, $e_3(\lambda_1)$ and $f_3(\lambda_1)$ as a consequence of the boundary condition equations. This way, one can construct three independent singular eigenfunctions having the classical $\frac{1}{\sqrt{r}}$-crack tip singularity. Six linearly independent functions as ingredients of these eigenfunctions will be identified and used as enrichment functions for the X-FEM.

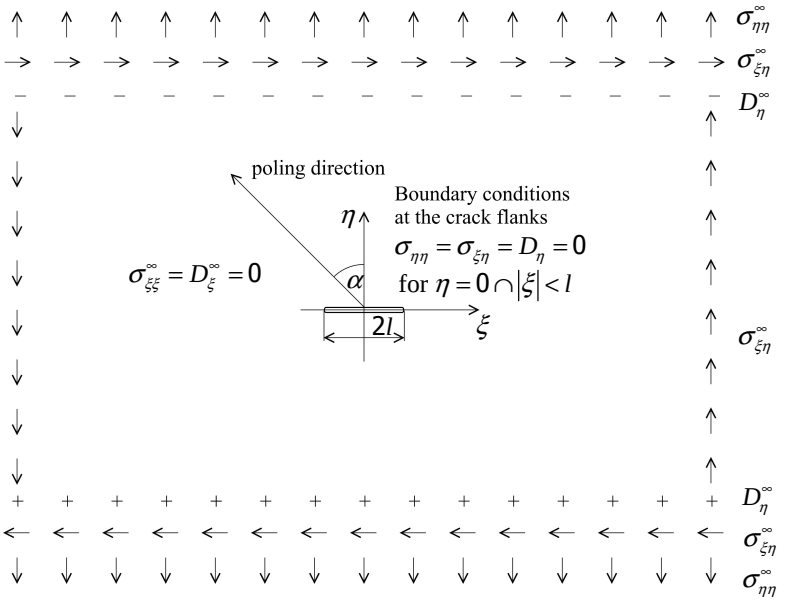

Figure 3. *Griffith crack inside an infinite piezoelectric solid*

3.2. *Analytical solutions for a center crack in an infinite medium*

In order to assess the influence of the piezoelectric enrichment functions and to study their convergency, we need a complete analytical solution for a crack within a certain boundary value problem. The use of the eigensolutions presented above, which belong to boundary value problems as well, is not advantageous in this context. This is because these solutions, or a part of them, will be applied as enrichment functions for the X-FEM. Thus, for proving the

developed numerical techniques it is necessary to use other independent analytical solutions. Here, solutions for a Griffith crack in an infinite piezoelectric medium will be used. The loads are given at infinity as shown at Figure 3.1. We apply transversely isotropic piezoelectric material with arbitrary poling direction α with regard to the crack.

Within this publication, we will give only a short explanation how the solution was constructed. Because of the crack as a geometrical object is not perpendicular to the poling direction, the material axes (x, y) used in the general solution of the Section 3.1 cannot be applied here. This way, one has to rewrite the material equations for the coordinate system (ξ, η) shown in Figure 2. In the same way as considered in Section 3.1, we get one partial differential equation of sixth order for the stress function $U(\xi, \eta)$ as a consequence of the compatibility equations. Further, one applies $U(\xi, \eta)$ in the form $U(\xi, \eta)$=$U(\xi + a\eta)$ and the resulting partial differential equation gives a more complicated characteristic equation for a having six roots: a_1, $\overline{a}_1$, a_2, $\overline{a}_2$, a_3 and $\overline{a}_3$. Exploiting the real valueness of $U(\xi + a\eta)$, the stresses and the dielectric displacements result in:

$$\sigma_{\xi\xi} = 2\mathbf{RE}\left(\sum_{k=1}^{3} a_k^2 \varphi_k(\zeta_k)\right), \sigma_{\eta\eta} = 2\mathbf{RE}\left(\sum_{k=1}^{3} \varphi_k(\zeta_k)\right)$$

$$\sigma_{\xi\eta} = -2\mathbf{RE}\left(\sum_{k=1}^{3} a_k \varphi_k(\zeta_k)\right)$$

$$D_\xi = 2\mathbf{RE}\left(\sum_{k=1}^{3} a_k \kappa_k \varphi_k(\zeta_k)\right), D_\eta = -2\mathbf{RE}\left(\sum_{k=1}^{3} \kappa_k \varphi_k(\zeta_k)\right) \quad [15]$$

RE denotes the real part of a complex number. In (15), the dependencies $\varphi_k(\zeta_k)$ stand for arbitrary holomorphic functions (Mußchelichwili, 1971) of the corresponding complex arguments $\zeta_k = \xi + a_k\eta$ with the characteristic roots a_k. It is clear that the analytic functions $\varphi_k(\zeta_k)$ are closely connected to the stress function U. κ_k are complicated functions of the material parameters, the angle α and the characteristic roots. Because of the complexity, the precise expressions of these functions will not be given here. Knowing the functions $\varphi_k(\zeta_k)$ the boundary value problem is solved. The deformations $\varepsilon_{\xi\xi}$, $\varepsilon_{\xi\eta}$, $\varepsilon_{\eta\eta}$ and the electric field E_ξ and E_η are defined from the stresses and the dielectric displacements by means of the material equations. The displacements and the electric potential follow after integration from $\varepsilon_{\xi\xi}$, $\varepsilon_{\xi\eta}$, $\varepsilon_{\eta\eta}$, E_ξ and E_η.

To guarantee the fulfilment of the boundary conditions at the crack flanks and the conditions at infinity (constant stresses and constant dielectric dis-

placements), it is obvious that the holomorphic functions $\varphi_k(z_k)$ must have the form:

$$\varphi_k(\zeta_k) = \frac{A_k \zeta_k}{\sqrt{\zeta_k^2 - l^2}} + B_k,\ A_k = A_k^{(\mathrm{re})} + \mathrm{i}A_k^{(\mathrm{im})},\ B_k = B_k^{(\mathrm{re})} + \mathrm{i}B_k^{(\mathrm{im})} \quad [16]$$

Equation [16] contains 12 arbitrary real constants ($A_k^{(\mathrm{re})}$, $A_k^{(\mathrm{im})}$, $B_k^{(\mathrm{re})}$, $B_k^{(\mathrm{im})}$, k=1,2,3) the specific values of which result from the boundary conditions given in Figure 3.1. The constant l means the half crack length. The determination of the mentioned real constants requires some complex algebraic manipulations, within which one has to take care for the exclusion of the rigid body motions and for the fixing of the electric potential with respect to a constant value. Because of the complexity, the concrete relations will not be given here, but they will be used as reference solution to be compared with the X-FEM.

4. The classical X-FEM formulation

As in the original article from Moës et al. (Moës *et al.*, 1999), the crack is described by a pair of level set functions. The classical enrichment function used for isotropic elastic materials are as following. They are derived from the asymptotic expansion for a semi-infinite crack in an infinite domain.

There are four basic enrichment functions ($C_1 = 1, 2, \cdots, 4$) needed to span the Westergaard-Williams-Sneddon solution (Sih *et al.*, 1968; Belytschko *et al.*, 1999) at the crack tip :

$$g_i^e(r,\theta) = \left\{ \sqrt{r}\sin\frac{\theta}{2}, \sqrt{r}\cos\frac{\theta}{2}, \sqrt{r}\sin\frac{\theta}{2}\sin\theta, \sqrt{r}\cos\frac{\theta}{2}\sin\theta \right\} \quad [17]$$

We won't enter into details here, the classical enrichment strategy for cracks in isotropic materials has been already described in numerous publications. We will compare the relative performance of this enrichment with the specific one described in the sequel.

5. New enrichment functions for cracks in piezoelectrics

The asymptotic expansion for a crack in an infinite piezoelectric medium has been derived in Section 3.1. From this expansion, we can determine a set of elementary functions that span the same functional space, for any supposed orientation of the crack. For plane problems, there are three independent eigenmodes (only two in the isotropic elasticity). These modes are combined in an arbitrary way and this for each spatial variable x or y. It should be noted that these functions depend on the orientation of the crack with respect to the material axes α, on the contrary to the isotropic case. Altogether, one needs six

functions to describe all the possible states at the crack tip, as opposed to the only four functions used to span the Westergaard-Williams-Sneddon solution in the isotropic elastic case. These independent functions are extracted from the asymptotic singular solution [12] and [13], derived in Section 3.1.

$$g_i^p(r,\theta) = \left\{\sqrt{r}f_1(\theta), \sqrt{r}f_2(\theta), \sqrt{r}f_3(\theta), \sqrt{r}f_4(\theta), \sqrt{r}f_5(\theta), \sqrt{r}f_6(\theta)\right\} \quad [18]$$

where:

$$\begin{aligned} f_i(\theta) &= \phi\left(\omega(\theta,\alpha), a_i^{(\mathrm{re})}, a_i^{(\mathrm{im})}\right) \\ &= \begin{cases} \rho\left(\omega, a_i^{(\mathrm{re})}, a_i^{(\mathrm{im})}\right)\cos\frac{\psi\left(\omega, a_i^{(\mathrm{re})}, a_i^{(\mathrm{im})}\right)}{2} & \text{if } a_i^{(\mathrm{im})} > 0 \\ \rho\left(\omega, a_i^{(\mathrm{re})}, a_i^{(\mathrm{im})}\right)\sin\frac{\psi\left(\omega, a_i^{(\mathrm{re})}, a_i^{(\mathrm{im})}\right)}{2} & \text{if } a_i^{(\mathrm{im})} \leq 0 \end{cases} \end{aligned} \quad [19]$$

The complex numbers $a_i = a_i^{(\mathrm{re})} + \mathrm{i}a_i^{(\mathrm{im})}$ are the six roots of the characteristic equation, and α is the orientation of the material axes with respect to the crack. The angles ω and ψ as well as the modified radius ρ have the form :

$$\begin{aligned} &\omega = \theta - \alpha \\ &\psi\left(\omega, a_i^{(\mathrm{re})}, a_i^{(\mathrm{im})}\right) = \frac{\pi}{2} + \pi\mathrm{int}\left(\frac{\omega}{\pi}\right) \\ &\qquad - \arctan\left(\frac{\cos\left(\omega - \pi\mathrm{int}\left(\frac{\omega}{\pi}\right)\right) + a_i^{(\mathrm{re})}\sin\left(\omega - \pi\mathrm{int}\left(\frac{\omega}{\pi}\right)\right)}{\left|a_i^{(\mathrm{im})}\right|\sin\left(\omega - \pi\mathrm{int}\left(\frac{\omega}{\pi}\right)\right)}\right) \\ &\rho\left(\omega, a_i^{(\mathrm{re})}, a_i^{(\mathrm{im})}\right) = \frac{1}{\sqrt{2}}\sqrt[4]{|a_i|^2 + a_i^{(\mathrm{re})}\sin 2\omega - \left(|a_i|^2 - 1\right)\cos 2\omega} \end{aligned} \quad [20]$$

In addition to this, the same enrichment function as in the case of isotropic elasticity is used to represent the jump in the displacement and in the electric potential. This whole set is then combined with regular FEM shape functions to build the approximation space for both the displacements $\mathbf{u}$ and the potential φ:

$$\mathbf{u}^h = \sum_{i\in R}\mathbf{N}_i\alpha_i + \sum_{i\in T}\sum_{j=1\ldots6}\mathbf{N}_i g_j^p\beta_{ij} + \sum_{i\in H}\mathbf{N}_i h\gamma_i \quad [21]$$

$$\varphi^h = \sum_{i\in R}N_i\zeta_i + \sum_{i\in T}\sum_{j=1\ldots6}N_i g_j^p\eta_{ij} + \sum_{i\in H}N_i h\xi_i \quad [22]$$

It is worth noting that the same enrichment functions are used for the displacements and the electric potential.

6. Convergence in the energy norm

The convergence is studied by comparing exact solutions for a reference problem to the actual results of a numerical model. The total (internal) energy of the system is given by:

$$W = \frac{1}{2} \int \left(c_{ijkl} \varepsilon_{ij} \varepsilon_{kl} + \kappa_{ij} E_i E_j \right) dV \qquad [23]$$

Let $\Delta\varepsilon_{ij} = \varepsilon_{ij} - \varepsilon_{ij}^{ex}$ be the difference in strains, and $\Delta D_i = E_i - E_i^{ex}$ be the difference in electrical field. The error in the (total) energy norm is then given by:

$$err_W = \sqrt{\frac{1}{2} \int c_{ijkl} \Delta\varepsilon_{ij} \Delta\varepsilon_{kl} + \kappa_{ij} \Delta D_i \Delta D_j dV}, \qquad [24]$$

where ε_{ij}^{ex} and E_j^{ex} are obtained from the exact displacement and electric fields u^{ex} and φ^{ex} that follow from the solution in Section 3.2. The error energy norm err_W does not contain terms involving the piezoelectric coupling e_{ijk}, because of symmetries. This would not have been the case if we had used the enthalpy H as reference, but convergence results shown in the sequel are also valid for H.

The example problem is that of a Griffith crack in an infinite medium, discussed in Section 3.2. Boundary conditions are applied at infinity. The computations were made with a FEM-model, whose mesh is structured and has been gradually refined. Of course the computational domain is finite, so we apply the exact solution for an infinite domain as boundary condition for the finite computational domain. The length of the crack is 8 and the domain is 32x32. The material axes have been rotated by an angle of 30 degrees with respect to the plane of the crack to avoid trivial symmetry of the solution.

We performed five sets of simulations with various enrichment strategies:

1) a topological enrichment done with six functions

2) a geometrical enrichment done with six functions

3) a geometrical enrichment done with six functions and a bigger enriched domain

4) a geometrical enrichment done with the four functions used in linear elasiticity

5) no enrichment at all

Figure 4 shows the relation between the mesh density and the error in the energy norm in a log-log scale. It should be stressed that any enrichment

strategy allows better results than without enrichment. This fact has been explained in earlier papers extensively, so we will not discuss it further. Thus, these results without enrichment are for reference only. What we would like to show here is the relative performance between a) a topological enrichment and a geometrical enrichment and b) an enrichment made with the six functions that are specifically designed for piezoelectric materials and the simple use of the four standard functions that are theoretically valid only for linear isotropic elasticity.

6.1. *Relative performance: Geometrical enrichment vs. topological enrichment*

Figure 4 shows that the convergence rate for geometrical enrichments is roughly double than that of the topological enrichment. This is what was expected (as shown in (Béchet *et al.*, 2005)) when the enrichment function well represents the physics of the phenomenon. Here, the six enriched function that were specifically developed for the piezoelectric crack are "doing the job" and hence allow to recover the classical convergence rate for finite elements with smooth problems (1.0 for linear elements). The drawback is an increased computational effort due to the bad conditioning of the resulting matrices. This has been discussed in (Béchet *et al.*, 2005) and solutions have been proposed to adress this issue.

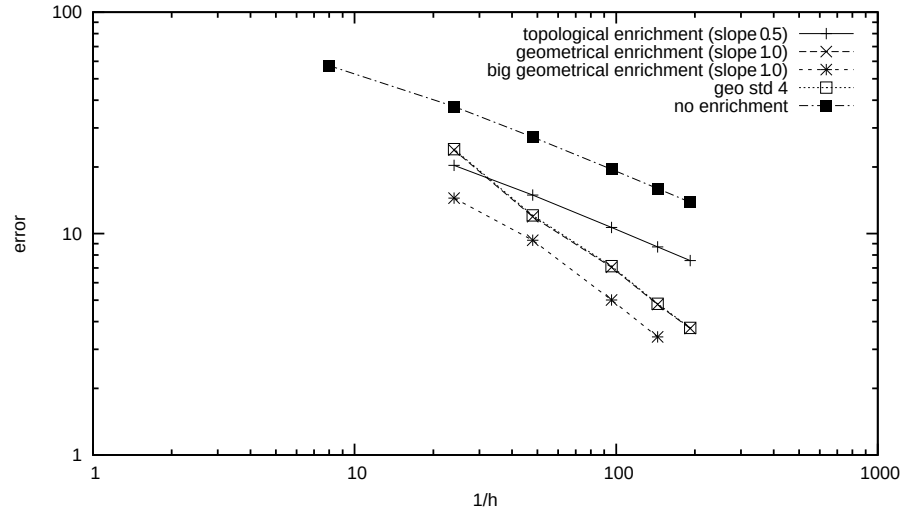

Figure 4. *Convergence for various enrichment strategies*

6.2. *Relative performance: 6-fold enrichment vs. 4-fold enrichment*

Comparing results obtained using a specifically designed 6-fold enrichment with the standard 4-fold enrichment of the isotropic elasiticity in similar settings, almost no difference is found. It means that the classical 4-fold enrichment spans a functional space that is large enough to represent well the more complex crack tip behaviour found in piezoelectrics. While this may be surprising, it must be tempered by the fact that piezos are not very far from having a isotropic behaviour both in the mechanical and electrical variables. Furthermore, the coupling which is clearly anisotropic has a very weak magnitude. Thus, the additional degrees of freedom and shape of the 6-fold enrichment may be of little advantage for piezos. This is not a bad news, since it means that reliable piezoelectric simulations can be made using the much simpler 4-fold enrichment.

7. Conclusions

We have devised an enrichment scheme based on the asymptotic expansion around a crack tip in piezoelectric materials. This enrichment scheme uses the six eigenfunctions of the asymptotic expansion. As such, it is optimal with regard to the problem to be solved (it contains the exact solution for a semi-infinite crack in an infinite body). However, a comparison made with the classical 4-fold enrichment that is used for isotropic elasticity is interesting. It shows that, with an accuracy higher than usually expected for engineering problems, the 4-fold enrichment is almost as efficient in the error in energy. This way, it is simpler to implement and involves less computational overhead, because it adds only 4 degrees of freedom (dofs) per regular dof, instead of six. For piezoelectric problems, it is therefore advisable to use the regular enrichment functions from the isotropic elasticity. It should be mentionned that similar results have been obtained previously (Elguedj *et al.*, 2005) with alternative enrichment functions for cracks in confined plasticity problems.

Acknowledgements

We wish to dedicate this work to the memory of M. Scherzer who has passed away shortly before this article was accepted.

8. References

Béchet E., Minnebo H., Moës N., Burgardt B., " Convergence and conditioning issues with X-FEM in fracture mechanics", *International Journal for Numerical Methods in Engineering*, vol. 64, p. 1033-1056, 2005.

Béchet E., Scherzer M., Kuna M., " Application of the X-FEM to the fracture of piezoelectric materials", *Submitted to International Journal for Numerical Methods in Engineering*, 2008.

Belytschko T., Black T., " Elastic crack growth in finite elements with minimal remeshing", *International Journal for Numerical Methods in Engineering*, vol. 44, p. 601-620, 1999.

Elguedj T., Gravouil A., Combescure A., " Appropriate extended functions for X-FEM simulation of plastic fracture mechanics", *Computer Methods in Applied Mechanics and Engineering*, vol. 195, n° 7-8, p. 501-515, 2005.

Moës N., Dolbow J., Belytschko T., " A finite element method for crack growth without remeshing", *International Journal for Numerical Methods in Engineering*, vol. 46, p. 131-150, 1999.

Mußchelichwili N., *Einige Grundaufgaben zur mathematischen Elastizitaetstheorie*, VEB Fachbuchverlag (Leipzig), 1971.

Osher S., Sethian J., " Fronts propagating with curvature-dependent speed: algorithms based on Hamilton-Jacobi formulations", *Journal of Computational Physics*, vol. 79, p. 12-49, 1988.

Scherzer M., Kuna M., " Combined analytical and numerical solution of 2D interface corner configurations between dissimilar piezoelectric materials", *International Journal of Fracture*, vol. 127, n° 1, p. 61-99, 2004.

Sih G., Liebowitz H., *Fracture,an advanced treatise*, vol. 2, Academic Press, London, UK, 1968.

Sosa H., " Plane problems in piezoelectric media with defects", *International Journal of Solids and Structures*, vol. 28, n° 4, p. 491-505, 1991.

Suo Z., Kuo C., Barnett D., Willis J., " Fracture mechanics for piezoelectric ceramics", *Journal of the Mechanics and Physics of Solids*, vol. 40, n° 4, p. 739-765, 1992.